

**Drifting mass accommodation coefficients: *in situ* measurements  
from a steady state molecular dynamics setup**

Yigit Akkus,<sup>1,\*</sup> Akif Turker Gurer,<sup>1</sup> and Kishan Bellur<sup>2</sup>

<sup>1</sup>*ASELSAN Inc., 06172 Yenimahalle, Ankara, Turkey*

<sup>2</sup>*Michigan Technological University, Houghton, MI 49931, USA*

(Dated: October 20, 2022)

arXiv:2003.01022v1 [physics.chem-ph] 17 Feb 2020

## Abstract

A fundamental understanding of the evaporation/condensation phenomena is vital to many fields of science and engineering, yet there is much discrepancy in the usage of phase change models and associated coefficients. We review kinetic theory of phase change from a fundamental standpoint and discuss the controversial mass accommodation coefficient, MAC ( $\alpha$ ), and its inconsistent definitions. The discussion focuses on the departure from equilibrium; represented as a macroscopic “drift” velocity. Constructing a continuous flow, phase change driven molecular dynamics setup, we investigate the steady state condensation at a flat liquid-vapor interface of Argon at various heating rates and temperatures. We calculate a value of MAC directly from the kinetic theory based Hertz-Knudsen (H-K) and Schrage (exact and approximate) expressions without the need for *a priori* physical definitions, *ad hoc* particle injection/removal or particle counting. MAC values from the approximate and exact Schrage expressions ( $\alpha_{app}^{Schrage}$  and  $\alpha_{exact}^{Schrage}$ ) are between 0.8 and 0.9 while MAC values from the H-K expression ( $\alpha^{H-K}$ ) was surprisingly above unity for all cases tested. All values of MAC reduce with saturation temperature in a manner consistent with prior studies.  $\alpha_{exact}^{Schrage}$  yields values closest to the results from transition state theory [*J Chem Phys*, **118**, 1392–1399 (2003)]. The departure from equilibrium (drift velocity, phase change rate) does not affect the value of  $\alpha_{exact}^{Schrage}$  but causes  $\alpha^{H-K}$  to vary drastically giving rise to the need for a velocity dependent correction. MAC values greater than unity violate conservation laws within the purview of commonly used physical definitions. Between multiple kinetic theory models and definitions, MAC values are not universal and cannot be interchangeably without appropriate correction factors. This explains the wide range of reported values. Even though a definition of MAC is not entirely necessary to model phase change, we hope that a standard definition of MAC be developed that is both consistent with kinetic theory and includes a physical description of the interfacial region.

**Keywords:** Mass accommodation coefficient, kinetic theory of phase change, Hertz-Knudsen equation, Schrage relationships, molecular dynamics

---

\* E-mail: yakkus@aselsan.com.tr

## I. INTRODUCTION

Classical kinetic theory is a statistical description of the behavior of gases based on velocities of the constituent molecules. Kinetic theory has provided the basis for modeling phase change in cases where the mass transport across the interface is not limited by the diffusion in the vapor phase. Under equilibrium conditions, the vapor in the vicinity of the liquid-vapor interface can be approximated as a perfect (ideal) gas and the velocity distribution of the vapor molecules follows a Maxwell Boltzmann distribution [1, 2]. This velocity distribution leads to an expression for the *maximum* collision frequency with a planar surface. Phase change is a dynamic process and a pure liquid-vapor system undergoes simultaneous condensation and evaporation. A net phase change flux is generally expressed as an algebraic sum of evaporation and condensation fluxes.

Mass accommodation coefficients (MAC) were introduced to account for deviation from the kinetic theory predicted *maximum* flux. The deviation is attributed to reflection of vapor molecules at the interface. There has been much discrepancy in both definition and reported values of MAC [3–5]. For example, Marek and Straub [4] reported a spread of 3 orders of in prior published values for water and Kryukov and Levashov [3] reported 3 different definitions of MAC. This is further complicated by the fact that additional modifications have been made to the original equations. Coefficients values reported from a particular kinetic theory expression cannot be used interchangeably with a different expression due to the lack of a standard definition for the coefficient. This reduces the coefficient to an empirical fitting parameter that is not universally applicable. Incognizance of fundamental assumptions is a possible reason for much controversy regarding both the applicability of kinetic theory expressions and the corresponding coefficients [5]. At this juncture, we feel that it is necessary to remind the reader and show without ambiguity the assumptions involved kinetic theory descriptions of phase change. In the rest of the section, we review the most common kinetic theory expressions from a fundamental standpoint and explore the prior published values of the accommodation coefficient.

### A. Kinetic Model for Liquid-Vapor Phase Change

Assuming the distribution of vapor molecules to be Maxwellian and treating the vapor as an ideal gas, the collision frequency of vapor molecules with a hypothetical plane surface in the vapor can be expressed as [6]:

$$j^V = \rho^V \sqrt{\frac{k_b T^V}{2\pi m}} \quad (1)$$

where  $\rho^V$ ,  $k_b$ ,  $m$ , and  $T^V$  are vapor density, Boltzmann constant, mass of a molecule, and vapor temperature, respectively. Mass flux crossing the hypothetical surface is given by  $j^V$ , where superscript  $V$  denotes the vapor phase.

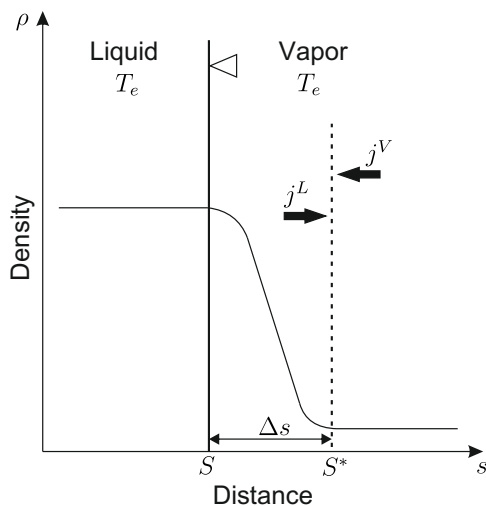


FIG. 1. Liquid-vapor interface at equilibrium. Solid vertical line demonstrates the interface defined based on the sharp interface approach. Vertical dash line is a hypothetical surface close to the sharp interface.

In order to extrapolate this expression to interphase mass transport such as a liquid-vapor system, we must first define the liquid-vapor interface. In many prior studies, the interface was assumed to be sharp [7]. Since Eq. 1 is theoretically only applicable in the vapor phase, a hypothetical surface ( $S^*$ ) close to the sharp interface ( $S$ ) on the vapor side is considered (Fig. 1) [2]. The condensation flux  $j^V$  is the number of vapor molecules crossing the surface  $S^*$  in the negative  $s$ -direction and the evaporation flux  $j^L$  is the number of vapor molecules crossing the surface  $S^*$  in the positive  $s$ -direction as shown in Fig. 1.  $S^*$  is assumed to be infinitesimally close to  $S$  but a formal description is lacking [2]. This causes considerable discrepancy in the evaluation of  $\rho^V$  and/or  $T^V$  since they could vary with  $s$ . In addition,

at the nanoscale, the concept of a Gibbs dividing surface is not valid. The liquid-vapor interface is diffuse and an “interfacial region” with a density gradient exists [3, 8–13]. In order to aid in both accuracy and consistency,  $S^*$  could be defined as the intersection of the interfacial region and the bulk vapor. The interfacial region thickness ( $\Delta s$ ) is generally less than 1 mean free path of the bulk vapor.

In equilibrium, the evaporation flux is equal to the condensation flux,  $j^V = j^L$ . There is no temperature jump across the interface and the liquid-vapor system is saturated. The vapor density in equilibrium is equal to the vapor saturation density at the corresponding saturation temperature. Hence,

$$j^V = j^L = \rho_{sat}^V(T_e) \sqrt{\frac{k_b T_e}{2\pi m}} \quad (2)$$

where superscript  $L$  and subscript  $e$  denotes the liquid phase and equilibrium, respectively.

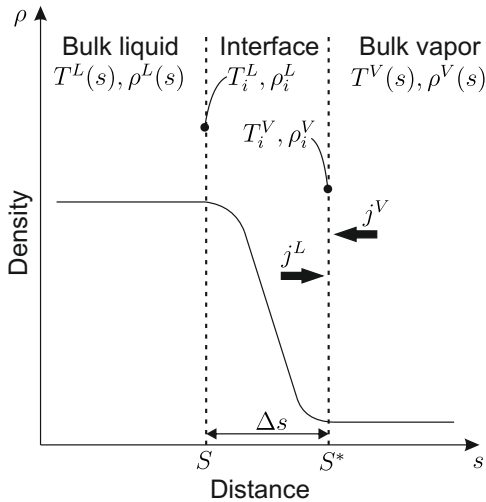


FIG. 2. Thermodynamic quantities used for the diffuse interface during net evaporation or condensation process.

During net evaporation or condensation,  $j^V$  and  $j^L$  are not equal. We entertain the possibility that the bulk vapor temperature could be different from the bulk liquid temperature and undergo a transition in the interfacial region similar to density (Fig. 2). Additionally, interfacial temperature and densities could be different from the corresponding bulk phase values. The interfacial properties are shown using a subscript  $i$ . A net phase change rate can be defined as the difference between the evaporation and condensation fluxes. The condensation flux ( $j^V$ ) can be expressed by Eq. (1). The estimation of the evaporation flux

is not straightforward. A common approach is to consider an absolute rate of evaporation based on a liquid-vapor system equilibrated at the liquid interfacial temperature ( $T_i^L$ ) [7]. The absolute rate of evaporation is then given by Eq. (2) where  $T_e$  is replaced by  $T_i^L$ . Although there are several arguments to support the equilibrium approach to estimate evaporation flux [2, 7], several authors have argued against it [14] making this a point of open debate.

Assuming the variations of temperature and density are also negligible in the vapor phase (i.e.  $T_i^V = T^V$  and  $\rho_i^V = \rho^V$ ), net phase change flux is an algebraic sum of evaporation and condensation flux and is given by Hertz relation [6]:

$$\dot{m}'' = \sqrt{\frac{k_b}{2\pi m}} \left( \rho_{sat}^V(T_i^L) \sqrt{T_i^L} - \rho^V \sqrt{T^V} \right) \quad (3)$$

where  $\dot{m}''$  is the net mass flux. In this formulation, condensation flux is dependent on the local thermodynamic quantities (density and temperature) on the vapor side while the evaporation flux is dependent on the same quantities but on the liquid side. In other words, in Hertz relation (Eq. (3)), the rates of the concurrent condensation and evaporation processes only depend on the properties of their respective phases. A common argument made to support this approximation is that  $\Delta s$  is infinitesimally small. If  $\Delta s$  is smaller than 1 mean free path then any molecule that evaporates from the bulk liquid must pass through  $S^*$  before interacting with a vapor molecule thereby preserving the liquid properties as it passes through  $S^*$ . As mentioned earlier, the ability to estimate evaporation flux based on liquid properties is attributed to an equilibrium assumption to obtain the absolute evaporation flux. The Hertz approach has been criticized since it actively decouples any interaction between the two fluxes [5]. In essence, the Hertz equation provides the theoretical maximum phase change flux possible since molecular reflection at  $S^*$  was not incorporated.

Early experiments [4, 15] consistently measured phase change rates lower than that predicted by the Hertz equation. This is generally attributed to reflection of vapor molecules at the interface. When a vapor molecule is incident on the interface, it can interact in three ways: (i) the molecule can condense (i.e., the vapor molecule is absorbed into the bulk of the liquid), (ii) the molecule can be reflected back into the vapor space or (iii) the molecule can displace a liquid molecule thereby undergoing a simultaneous condensation-evaporation process. Vapor reflection reduces both the condensation and evaporation mass flux. In order to account for this deviation from the theoretical maximum (Eq. (3)), evaporation

and condensation coefficients were introduced [16] and the result is widely known as the Hertz-Knudsen equation:

$$\dot{m}'' = \sqrt{\frac{k_b}{2\pi m}} \left( \alpha_e \rho_{sat}^V(T_i^L) \sqrt{T_i^L} - \alpha_c \rho^V \sqrt{T^V} \right) \quad (4)$$

where  $\alpha_e$  is the evaporation coefficient and  $\alpha_c$  is the condensation coefficient.

### Coefficient definition(s)

Before any discussion of the coefficient values, we must first develop a definition. There is much inconsistency in the definition of the coefficients reported by prior studies. Most prior definitions could be grouped into 5 major categories:

**Definition 1:** Ratio of measured rate to calculated rate [9, 10, 15, 17–20].

**Definition 2:** Probability of capture or absorption [21–27].

**Definition 3:** Ratio of condensed molecules to incident molecules [11–13, 28–32].

**Definition 4:** Correction factor for quality of phase boundary [8].

**Definition 5:** Efficiency of molecules adhering to or abandoning the surface [33].

**Definition 1** inherently makes the coefficient dependent on kinetic theory and is not tied to a physical description. The measured rate is compared to the kinetic theory predicted rate and the coefficient is determined by comparison. This is convenient when using experiments to determine the coefficient. However, when molecular dynamics or other purely computational methods are used, other definitions are generally utilized. **Definitions 2–5** are independent of kinetic theory of phase change. The biggest open debate is whether the coefficient is an intrinsic property of the liquid-vapor system or just a fudge factor to kinetic theory expressions.

Let us consider the case where **Definition 1** is used to calculate the coefficient. The primary complication in evaluating Eq. (4) is that the interfacial liquid temperature ( $T_i^L$ ) and both kinetic coefficients are unknown. Even if  $T_i^L$  is measured or approximated, there remain two unknowns,  $\alpha_c$  and  $\alpha_e$ , in the expression for  $\dot{m}''$ . For sake of closure it is common practice to assume that the condensation coefficient is equal to the evaporation coefficient

( $\alpha_c = \alpha_e = \alpha$ ) [4, 22, 32, 34–41]. Under this assumption the only remaining coefficient in Eq. (5) is  $\alpha$ , which is referred to as the *mass accommodation coefficient (MAC)*. We call Eq. (5), a simplified version of Hertz-Knudsen equation (Eq. (4)), as simply Hertz-Knudsen (H-K) equation in the rest of the current study for brevity.

$$\dot{m}'' = \alpha \sqrt{\frac{k_b}{2\pi m}} \left( \rho_{sat}^V(T_i^L) \sqrt{T_i^L} - \rho^V \sqrt{T^V} \right) \quad (5)$$

A popular form of the Hertz-Knudsen equation is given below:

$$\dot{m}'' = \alpha \frac{1}{\sqrt{2\pi R}} \left( \frac{p_{sat}|_{T_i^L}}{\sqrt{T_i^L}} - \frac{p^V}{\sqrt{T^V}} \right) \quad (6)$$

where  $p$  is pressure and  $R$  is the specific gas constant. This is equivalent to Eq. (5) when an ideal gas approximation is made to convert densities to pressures. This poses a concern since phase change is an inherent non-equilibrium process. The velocity distribution has the potential to deviate from the equilibrium Maxwellian which makes the applicability of the ideal gas expression to the vapor close to the interface is suspect. In this study we retain the original density form of the kinetic theory expression and introduce modifications to account for potential departure from equilibrium.

#### Departure from equilibrium

Under equilibrium conditions, the evaporation flux is equal and opposite to the condensation flux (i.e. the net flux is zero) and the velocity distribution is a perfect Maxwellian. Phase change is an inherently non-equilibrium process and Schrage [7] argued that during steady phase change there is a net macroscopic velocity of the vapor molecules either towards or away from the interface. This is also referred to as a “drift” velocity. Drift velocity was superimposed with the Maxwell Boltzmann distribution to develop a correction factor ( $\Gamma$ ). Schrage’s formulation can be expressed as,

$$\dot{m}'' = \alpha \sqrt{\frac{m}{2\pi k_B}} \left( \frac{\rho_{sat}|_{T_i^L}}{\sqrt{T_i^L}} - \Gamma(a) \frac{\rho^V}{\sqrt{T^V}} \right) \quad (7a)$$

where  $a$  is the ratio of the drift velocity ( $w_0$ ) to the mean thermal velocity of the vapor

molecules (Eq. (7b)) and  $\Gamma$  is the correction factor (Eq. (7c)):

$$a = \frac{w_0}{\sqrt{2k_B T^V/m}} \quad (7b)$$

$$\Gamma(a) = \exp(-a^2) - a\sqrt{\pi}[1 - \text{erf}(a)] \quad (7c)$$

where  $w_0$  is the drift velocity in Eq. (7b) and is given by  $w_0 = \dot{m}''/\rho^V$ , where  $\rho^V$  is the vapor density. If the drift velocity is small in comparison to the thermal velocity, Eq. (7c) reduces to  $\Gamma(a) \approx 1 + a\sqrt{\pi}$  [2]. If the ideal gas expression is used to evaluate  $\rho^V$ , then, in the limit of small  $a$ , the original Schrage expression (Eq. (7a)) can be reduced to Eq. (8) [2, 21, 32].

$$\dot{m}'' = \frac{2\alpha}{2 - \alpha} \sqrt{\frac{m}{2\pi k_B}} \left( \frac{\rho_{sat}|_{T_i^L}}{\sqrt{T_i^L}} - \frac{\rho^V}{\sqrt{T^V}} \right) \quad (8)$$

While the kinetic factor in H-K equation (Eq. (5)) is simply  $\alpha$ , it is  $2\alpha/(2 - \alpha)$  in the approximate Schrage expression <sup>1</sup> (Eq. (8)). A few researchers assume  $\alpha=1$  in Eq. (5) while others assume the same but in Eq. (8) [42–49]. In such a case, the approximate Schrage expression (Eq. (8)) would predict twice the mass flux predicted by H-K equation (Eq. (5)) for the same value of  $\alpha = 1$ . A value of unity is just a theoretical upper limit (i.e., it is the limit predicted by Hertz relation, Eq. (3)) and most prior studies have reported values less than unity [4].

## B. Prior measurements of MAC

Experimentally determined values of MAC have been highly inconsistent [4, 36, 50]. For water alone, the reported values vary by almost three orders of magnitude [4]. To determine MAC from experiments,  $\dot{m}''$  and  $T_i^L$  must be measured with a high degree of accuracy and this poses several experimental challenges; the first of which is the existence of large temperature jumps at the interface [5]. Second, if the interface is not perfectly flat, additional factors could alter both  $\dot{m}''$  and  $T_i^L$  considerably [51]. Lastly, the presence of impurities further alters the shape of the interface and thereby the local properties. The

<sup>1</sup> A majority of papers erroneously refer to Eq. (8) as the original Schrage expression. Although it is derived from the original equation developed by Schrage [7], there are two inherent assumptions: (i) the drift velocity of the vapor molecules is small in comparison to the mean thermal velocity, and, (ii) ideal gas equation is used to evaluate vapor density.

experimental discrepancy in prior measured values of MAC have been attributed to difficulty in measuring interfacial temperature, dynamic surface tension, renewing/re-wetting surfaces and trace impurities in the liquid [4, 36, 50].

Molecular dynamics (MD) simulations are an alternative to mitigate the aforementioned experimental challenges and have been widely used to investigate the phase change phenomenon. Consequently, a massive body of literature exists for the prediction of MAC by MD simulations. In this part, we try to highlight several influential studies.

Adopting **Definition 1** for the calculation of MAC, Yasuoka, Matsumoto, and Kataoka [9, 10] estimated MAC values for the condensation of argon and methanol as  $\sim 0.8$  and  $\sim 0.2$ , respectively, in their equilibrium simulations. Later, Matsumoto [18] reported MAC values for non-equilibrium simulations and pointed out the inverse relation between MAC values and the temperature. This dependence was also reported in many subsequent studies [11, 18, 19, 24, 27, 31, 32, 52–55]. In another study [30] conducting non-equilibrium MD simulation, MAC value of argon during condensation was reported around 0.82 across various surface tensions of the liquid interface. Tsuruta *et al.* [29, 56] investigated condensation probability of argon atoms, which were injected to the system and targeted to a condensing surface, and came up with a velocity dependent coefficient formulation ( $\sigma_c$ ) for the condensation of individual argon atoms. Then using transition state theory [11, 24], they reported a general expression for the average condensation coefficient of all atoms ( $\overline{\sigma_c}$ ) expressed by the specific volume ratio between liquid and vapor (translational length ratio). Our results are compared to the values found by using their formulation later in Section III C. Cheng *et al.* [27] conducted MD simulations to show the effects of molecular composition on the evaporation. They reported values for a single coefficient, namely condensation coefficient on an evaporating interface, and demonstrated that dimers and trimers had higher coefficients than monomers. However, coefficients were demonstrated to collapse onto a master curve when plotted against a translational length ratio, a concept suggested by Nagayama and Tsuruta [11]. Meland *et al.* [12] reported evaporation ( $\alpha_e$ ) and condensation ( $\alpha_c$ ) coefficients of LJ-spline fluid on both condensing and evaporating interfaces. They showed that these coefficients are not equal outside the equilibrium and depends on the drift velocity. Nagayama *et al.* [55] investigated the condensation/evaporation coefficients of some straight-chain alkanes (butane, dodecane, and octane) and estimated values consistent with the transition state theory.

Two studies of Holyst *et al.* [20, 41] attracted the attention of the community by reporting MAC values higher than unity. Authors adopted **Definition 1** for the calculation of MAC value and used Eq. (6) to estimate the theoretical prediction of the phase change rate. However, they assumed thermal equilibrium at the interface ( $T_i^L = T^V$ ). In 2016, Persad and Ward [5] published an extensive review on the evaporation and condensation coefficients and discussed commonly used simplifying assumptions during the estimation of these coefficients, among which the thermally equilibrated interface was criticized since the temperature discontinuity has been already revealed in many experimental and numerical studies. Persad and Ward [5] also introduced relations for evaporation and condensation coefficients based on statistical rate theory of quantum mechanics and demonstrated that coefficient values are not bounded by unity. They concluded that H-K relation is incomplete due to the decoupling of the two interacting phases.

A number of prior molecular dynamics studies calculated the coefficient by tracking particles that cross a hypothetical plane and determining the rate of reflection [9–11, 24, 27, 29, 32, 56]. This method raises concerns over the appropriateness of the time period for which the particle is tracked and the location of the hypothetical plane with respect to the interfacial region. Cheng *et al.* [27] referred to picking the time period as an *ad-hoc* approach. Calculation of MAC using molecular dynamics in the past has been primarily through use of equilibrium simulations [9–11, 18, 29, 55–57]. As discussed earlier, an equilibrium approach results in a net zero phase change flux and a net zero drift velocity. Hence, using an equilibrium molecular dynamics approach does not include the effect of drift velocity on phase change. Under non-equilibrium conditions the MAC determined by particle tracking could be different from those at equilibrium [12] and a velocity correction in the vapor is necessary [32]. Lastly, while a considerable number of non-equilibrium MD setups in previous studies were inherently transient [24, 27, 32, 52, 53, 58, 59], the ones with the steady state phase change process [12, 20, 41, 60] used *ad hoc* methods such as removing and/or injecting particles at prescribed regions of the simulation domain to sustain the continuous phase change process.

### C. Current study

Extreme caution must be used when using coefficients estimated through equilibrium simulations or particle tracking methods in kinetic theory expressions for three reasons: i) there is huge ambiguity in the definition of the coefficients and prior published values lack universal applicability to all kinetic theory based expressions, ii) departure from equilibrium and the effect of drift velocity must be accommodated either by both the simulation technique and the kinetic theory expression, and iii) the kinetic theory approach to phase change is built on multiple assumptions (that involves decoupling of two actively interacting phases [5]), and the simulation may not take this into account. The above problems can be avoided if the coefficients are back-calculated from H-K or Schrage's relation using data from a non-equilibrium, steady state molecular dynamics simulation. Since these equations are used in many engineering applications, obtaining coefficients that have direct applicability in these kinetic theory expressions is critical.

We aim to present the first NEMD study calculating the coefficients in a real steady state manner without the need for *ad hoc* particle injection/removal methods. Instead of assuming a definition for MAC and attributing it as a function of the drift velocity, we compute the absolute value of MAC by direct comparison of data from a non-equilibrium, steady state MD simulation with kinetic theory models of phase change (H-K and Schrage). Based on the results we discuss the validity of the different definitions for MAC and outline the effect of drift velocity on coefficients derived from both H-K and Schrage expressions.

## II. METHODOLOGY

Phase change driven nanopump technique, an MD simulation proposed by Akkus and Beskok [61] and utilized in different applications [62–64], is used to investigate the steady state condensation process at a flat liquid-vapor interface. The computational setup consists of two parallel walls composed of Platinum (Pt) atoms (gray spheres in Fig. 3). In the transverse direction, size of the simulation domain is determined by the outermost Pt layers of each wall. In the longitudinal direction, simulation domain extends substantially beyond the walls. When Argon (Ar) atoms are introduced into the system (blue spheres in Fig. 3a), they preferentially condense in the space between the two walls and forms a liquid bridge

due to the attraction of Ar atoms with the wall atoms. Ar atoms are placed asymmetrically in the computational domain such that when condensed into liquid phase, one of the free surfaces are pinned between the edges of the walls by means of capillarity, while the other free surface forms away from the wall edges at the opposite side, thereby creating a liquid slab as shown in Fig. 3a. The number of Ar atoms to be introduced is selected such that the thickness of the liquid slab attached to the walls at one end is appreciably higher than 2.5 nm, which was reported as a limit for the presence of the effects of disjoining pressure [58]. The rest of the simulation domain is occupied by the vapor phase of Ar. Periodic boundary conditions are applied in all directions. Periodicity in transverse direction renders the system analogous to a liquid block placed on a semi-infinite wall within a sufficiently large vapor medium. Moreover, sufficient thickness of the liquid slab prevents the formation of a curved interface at the free surface. Consequently, a flat interface is achieved at the surface of the liquid slab. This allows for direct applicability of kinetic models of phase change at planar interfaces.

## A. Simulation steps

### 1. *Thermostat application period*

To stabilize the system at the prescribed temperature, constant NVT ensemble (constant atom number, volume, and temperature) is applied to all atoms by the Nosé-Hoover thermostat method for 60 ns except the atoms in outermost layers of the walls, which are always fixed at their lattice positions to preserve the shape of the system.

### 2. *Equilibration period*

Following the thermostat application, microcanonical (NVE) ensemble (constant atom number, volume, and energy) is applied to Ar atoms for 120 ns to equilibrate the system. During this equilibration period, wall atoms are still subjected to the thermostat. At the end of this stage, thermally equilibrated and statistically stable liquid-vapor mixture is achieved. With time averaging, liquid-vapor interfaces become apparent in the system as shown in Fig. 3b. To determine the thermodynamic properties of the saturated fluid in the

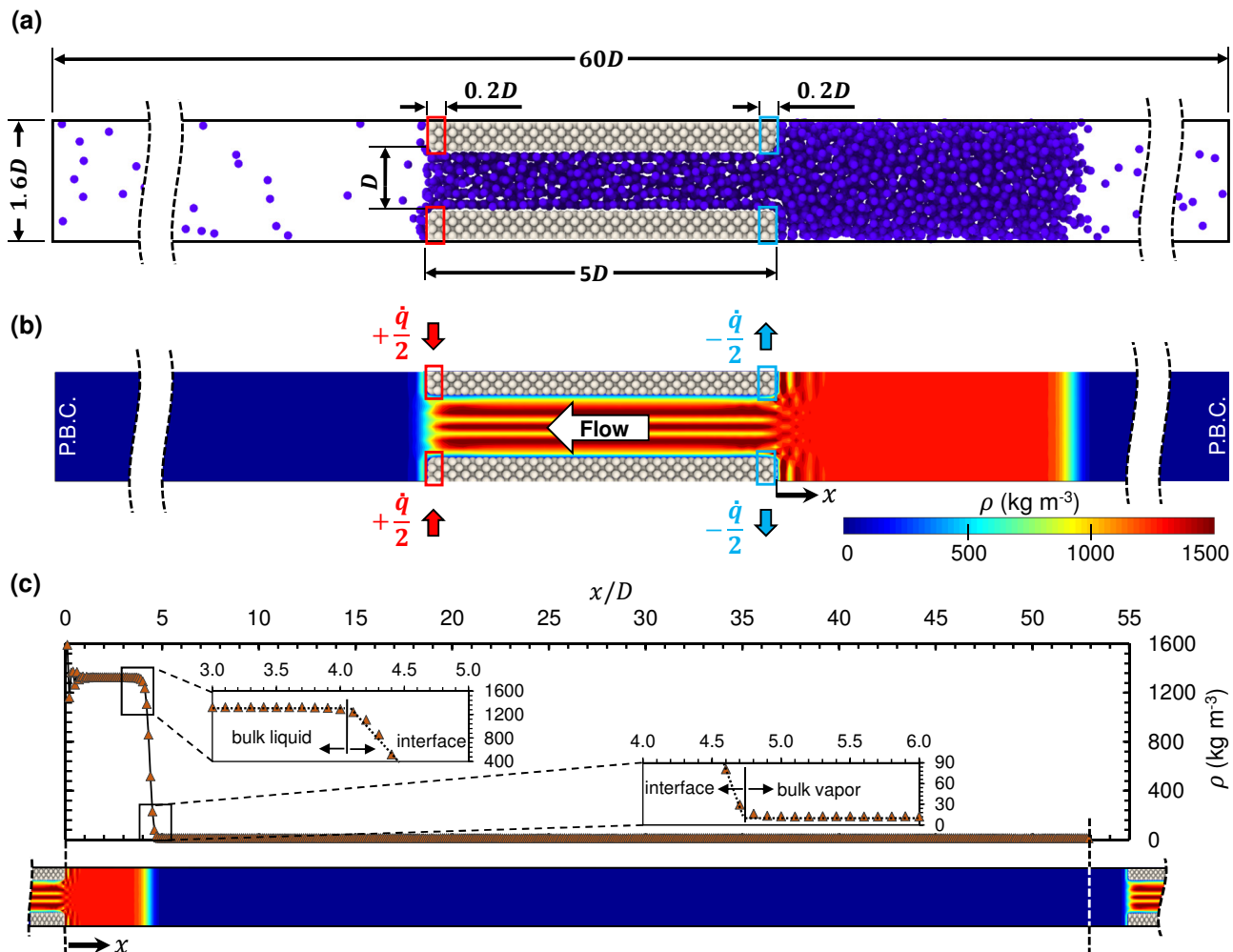


FIG. 3. (a) A snapshot of the computational setup at 90 K. Distance between the channel walls ( $D$ ) is 1.96 nm and the other dimensions in the simulation domain are proportional as shown in the figure. Depth of the simulation domain is 3.72 nm. The walls are composed of four atom layers and have a thickness of 0.59 nm. (b) 2-dimensional density distribution of the fluid (argon) after sufficient time averaging of MD results. Molecular layering, an experimentally observed phenomenon [65, 66] resulting from wall-force-field effect is apparent in the liquid phase between the walls. Red and blue rectangles enclose the solid atoms, which are subjected to the equal energy injection and extraction processes, respectively. (c) 1-dimensional density distribution of the fluid in longitudinal direction. Vertical bins with a thickness of  $0.1D$  are used to calculate the average density along  $x$ -direction, which starts at the side edges of the walls near the condenser side. Periodicity at the side boundaries enables a continuous gas phase along the  $x$ -direction. Data collection is ceased at a distance of  $2D$  from the evaporating interface to eliminate the possibility of any density variation in the vapor phase. Insets show the close-up view of the density distribution near the intersections of interfacial region with the bulk liquid and vapor phases.

present computational setup, data are collected from the equilibrated system during this stage.

### 3. Heating and cooling period

At the liquid-vapor interfaces of the equilibrated system, simultaneous evaporation and condensation of fluid atoms take place; however, the net rate of phase change is always zero. In order to create an interface with a net phase change rate, an energy exchange mechanism with the interface should be established. This mechanism is created by equally heating and cooling the solid atoms at the opposite ends of the nanochannel shown in Fig. 3 by red and blue rectangles, respectively, while Ar atoms are subjected to microcanonical (NVE) ensemble. Cooled atoms in the liquid slab lead to the net condensation while at the other end, the pinned interface is heated leading to a net evaporation. Condensed atoms are transported from the condensing interface to the evaporating interface *via* both Laplace pressure difference and molecular/atomic diffusion through the nanochannel [61]. In the absence of a meniscus, molecular/atomic diffusion near the walls (associated with the solid-liquid surface tension gradient [62, 67]) is responsible for the pumping of the liquid. Periodic boundary conditions enable the steady and continuous flow of Ar not only in liquid phase but also in vapor phase. Therefore, the system behaves like a nanopump, continuously pumping the fluid in a prescribed direction with zero overall heat transfer due to equal heating and cooling. Utilization of the nanopump technique to create a statistically stable, flat interface with steady interfacial mass transfer makes the current computational setup unprecedented. This truly steady state setup does not utilize any *ad hoc* treatment to sustain the steady operation and enable collecting data without any time restriction. In the present study, data are collected for 600 ns during the phase change. However, this duration can be further increased to reduce the uncertainty associated with the data.

#### B. Molecular simulation details

The numbers of fluid (Ar) and solid (Pt) atoms are 3783 and 4080, respectively. Walls are composed of 4 solid layers with (1,0,0) crystal planes facing the liquid. Lennard-Jones (L-J) 6-12 potential is used for the interactions between Ar-Ar and Ar-Pt. The interaction parameters utilized are:  $\sigma_{Ar} = 0.34$  nm,  $\sigma_{Ar-Pt} = 0.3085$  nm, and  $\varepsilon_{Ar} = 0.01042$  eV,  $\varepsilon_{Ar-Pt} = 0.00558$  eV [68]. Cut-off distance for the truncation of the L-J potential is selected as  $3\sigma_{Ar}$ . Embedded atom model is utilized to model Pt-Pt atomic interactions [69]. In order

to eliminate the non-physical temperature jump caused by thermostats [70], heat transfer to/from fluid is performed by energy injection/extraction from selected solid atoms instead of thermostat application. Wall atoms located between heating and cooling zones are not allowed to vibrate to eliminate the undesirable heat conduction through the walls, otherwise the majority of energy is transferred *via* the solid medium, which is much more conductive than the fluid. Simulations are initiated from the Maxwell-Boltzmann velocity distribution for all atoms. A time step of 5 fs is used throughout the simulations. The simulation data (i.e. density, temperature, and velocity) are averaged for 5 ns. Simulations are carried out using Large-scale Atomic/Molecular Massively Parallel Simulator (LAMMPS) [71].

### C. Interface detection

In the absence of the wall-force-field effect (i.e. away from the walls), density distribution of the fluid along the transverse direction is homogeneous. The liquid-vapor interface is intentionally positioned away from the walls (nearly  $27\sigma_{Ar}$ ) by adjusting the number of atoms used in the simulations. Both the interfacial region and the bulk vapor phase are free from any density variation in the transverse direction. Therefore, vertical bins are used to calculate the 1-dimensional distribution of density (see Fig. 3c) along the longitudinal direction. Liquid-vapor interfacial region is characterized by a density gradient. A piecewise fit to the density profile is made considering the bulk phases and the center of the interfacial region. The interfacial region is delineated by intersections of the extrapolated piecewise fits similar to the approach in Meland *et al.* [12]. These denote points of inflection (i. e. change in slope) of the density profile. (see the insets in Fig. 3c).

### D. Calculation of MAC values

Mass accommodation coefficients are calculated directly from the kinetic models of phase change (see Section I A): i) H-K equation (Eq. (5)), ii) exact Schrage relation (Eq. (7)), and iii) approximate Schrage relation (Eq. (8)). As stated earlier, these equations are generally expressed in terms of pressure and temperature. However, the pressure, especially in the liquid phase, is subjected to considerable fluctuations [30, 72, 73], which negatively affects the estimation of pressure. On the other hand, estimation of density is more reliable and

straightforward. Further, the original kinetic theory formulation was based on density and we preserve the original formulation here without an ideal gas assumption. It should be noted that these of these equations (Eqs. (5)–(8)) were developed for a net evaporation rate. We consider only the flat condensing interface in this study. Hence, the equations are re-arranged for net condensation:

$$\dot{m}'' = \alpha^{H-K} \sqrt{\frac{k_B}{2\pi m}} \left( \rho^V \sqrt{T^V} - \rho_{sat}|_{T_i^L} \sqrt{T_i^L} \right) \quad (9)$$

$$\dot{m}'' = \alpha_{exact}^{Schrage} \sqrt{\frac{k_B}{2\pi m}} \left( \Gamma(-a) \rho^V \sqrt{T^V} - \rho_{sat}|_{T_i^L} \sqrt{T_i^L} \right) \quad (10)$$

$$\dot{m}'' = \frac{2\alpha_{app}^{Schrage}}{2 - \alpha_{app}^{Schrage}} \sqrt{\frac{k_B}{2\pi m}} \left( \rho^V \sqrt{T^V} - \rho_{sat}|_{T_i^L} \sqrt{T_i^L} \right) \quad (11)$$

where mass accommodation coefficients (MACs) are designated according to the equations, in which they are used: i)  $\alpha^{H-K}$  is the MAC for Hertz-Knudsen equation, ii)  $\alpha_{exact}^{Schrage}$  is the MAC for exact Schrage relation, and iii)  $\alpha_{app}^{Schrage}$  is the MAC for approximate Schrage relation. These MACs can be explicitly calculated based on their respective equations as follows:

$$\alpha^{H-K} = \dot{m}'' \sqrt{\frac{2\pi m}{k_B}} \left( \rho^V \sqrt{T^V} - \rho_{sat}|_{T_i^L} \sqrt{T_i^L} \right)^{-1} \quad (12)$$

$$\alpha_{exact}^{Schrage} = \dot{m}'' \sqrt{\frac{2\pi m}{k_B}} \left( \Gamma(-a) \rho^V \sqrt{T^V} - \rho_{sat}|_{T_i^L} \sqrt{T_i^L} \right)^{-1} \quad (13)$$

$$\alpha_{app}^{Schrage} = \frac{2\alpha^{H-K}}{\alpha^{H-K} + 2} \quad (14)$$

where  $\rho^V$  and  $T^V$  are calculated by averaging the values in the gas phase.  $T_i^L$  is calculated at the exact point of the intersection of liquid phase and interfacial region (see Fig. 3c). Drift velocity ( $w_0$ ) is evaluated by averaging the  $x$ -component of the vapor atoms in a large bin placed in the bulk gas phase. Mass flux ( $\dot{m}''$ ) is calculated by multiplying the drift velocity with the gas density evaluated at the same bin.

### III. RESULTS AND DISCUSSION

#### A. Equilibrium simulations

At the nanoscale, interfacial and surface forces start to dominate over body forces, which leads to the severe deviations from continuum predictions. Near the close vicinity of the walls, molecular layering (density fluctuations) within the liquid is observed[65, 66]. Bulk fluid properties such as viscosity [74] and density [75] deviate from their bulk fluid properties. Moreover, free molecular flow or transition regime may be present in vapor phase if the mean free path of a molecule/atom is comparable to the size of the nano-conduit. Considering all these factors, equilibrium properties of a fluid in a nanoscale system can be dependent on the system itself. Therefore, saturated fluid properties of argon in our computational setup are determined from our equilibrium simulations similar to the approaches in previous studies [20, 32]. Figure 4 shows the density values of vapor obtained from 24 equilibrium simulations conducted in different temperatures. Equilibrium (saturation) vapor density is estimated from a fourth order polynomial fit to the data.

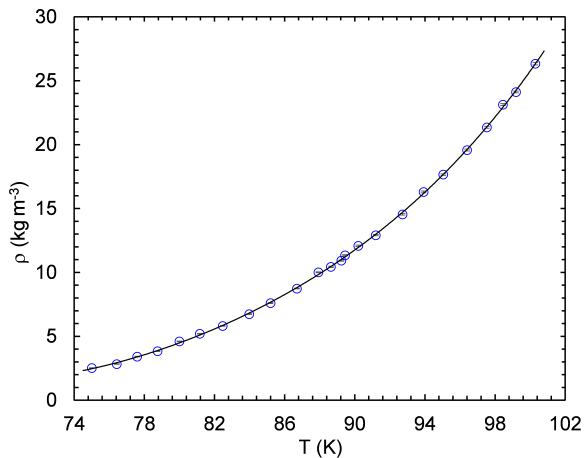


FIG. 4. Saturated vapor density of argon as a function of temperature. Blue circles are data points and the uncertainty of the data is smaller than the size of the circles. Solid line is the fourth order polynomial fit to the data. Addition of further data points has negligible effects on the polynomial fit.

## B. Near-equilibrium simulations

Using Eqs. (12)–(14), MAC values are determined for three systems, first equilibrated at the temperatures of 80 K, 90 K and 100 K, then subjected to small cooling/heating rates ( $\dot{q} = 0.2 - 0.6$  nW) during near-equilibrium simulations. Resultant MAC values on the condensing interface are reported in Fig. 5 as a function of the condensation rate.

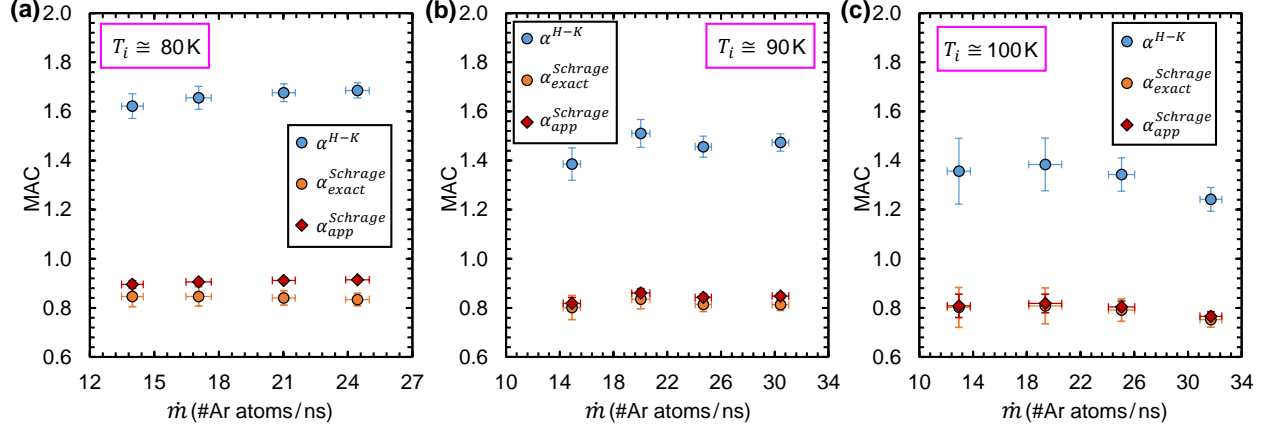


FIG. 5. Mass accommodation coefficients vs. condensation rate during near-equilibrium (small condensation rate) simulations.

During near-equilibrium condensation simulations, Schrage’s exact and approximate relations yielded MAC values around 0.8-0.9. H-K equation, on the other hand, yielded MAC values between 1.3-1.7. A value higher than unity appears to contradict physical definitions (**Definitions 2-5** discussed earlier) of MAC. The most commonly used **Definition 3** suggests that if MAC is higher than 1, the condensed flux is greater than the incident flux which is a violation of mass conservation.  $MAC > 1$  may be attributed to: (i) the assumed equality of coefficients; a simplification made on the original H-K equation (Eq. (4)), or (ii) neglect of drift velocity or (iii) an incorrect definition of MAC. However, values exceeding unity were reported even if the evaporation and condensation coefficients were not assumed to be equal [5]. Drift velocity correction proposed by Schrage always yields MAC values smaller than unity in our simulations. MAC values computed from both exact and approximate Schrage relations in the current study is in good agreement with the values reported in the literature [9, 11, 19, 29, 30].

Two trends are evident from Fig. 5. First, the coefficients calculated from approximate and exact Schrage relations become closer with increasing interface temperature. This is due

to the decrease in the value of  $a$ , the ratio of drift velocity to the mean thermal velocity. The approximate Schrage relation depends on the assumption of small  $a$ . With the increasing equilibration temperature, while the speed of vapor decreases due to increasing density, vapor temperature increases. These both effects decrease the value of  $a$  thereby increasing the validity of the approximate Schrage relation at higher temperatures. Second, MAC decreases with increasing temperature. This observation is well-known and reported many times in the literature [11, 18, 19, 24, 27, 31, 32, 52–55]. Figure 6 demonstrates MAC values as functions of interfacial liquid, interfacial vapor, and average interface temperatures:

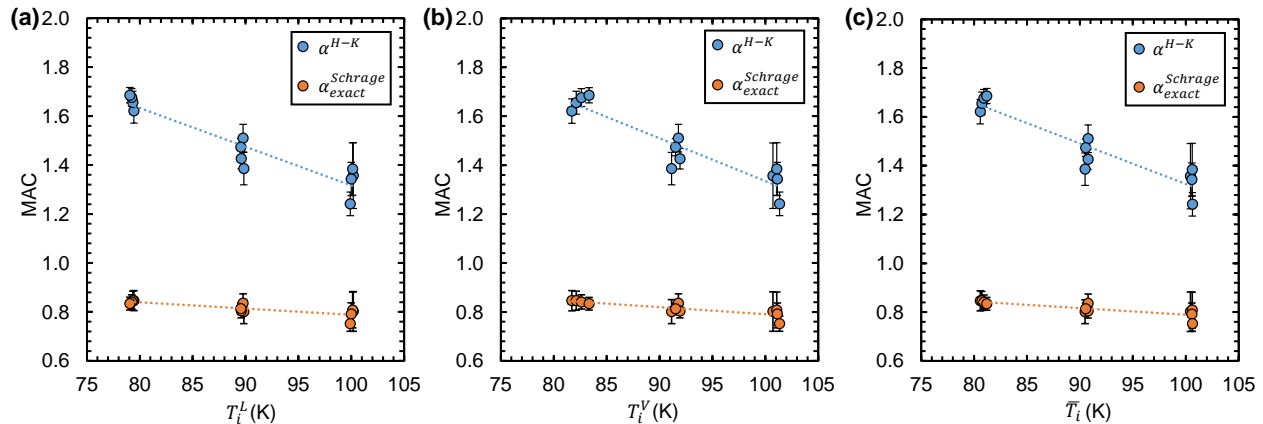


FIG. 6. Mass accommodation coefficients as the functions of (a) interfacial liquid temperature, (b) interfacial vapor temperature, and (c) average interface temperature. Dot-lines show the linear fit to the data.

MAC values predicted by the current study decrease with increasing temperature as expected. There is a strong temperature dependence in MAC calculated from the H-K equation, while a weak dependence is observed for MAC values calculated from the exact Schrage equation. MAC values calculated from the approximate Schrage equation have an intermediate dependence and they are not given in Fig. 6 for brevity.

### C. Non-equilibrium simulations

Although the derivation of kinetic models is dependent on a near-equilibrium assumption, these equations are still used by researchers and engineers to estimate the phase change rate in various applications. Therefore, we determined the MAC values even for the cases while phase change rate was not low. After the equilibration period, non-equilibrium simulations are conducted with the cooling (and heating) rates of  $\dot{q} = 0.7 - 4.0$  nW. Surprisingly, we find

that some of the MAC values vary with the heating/cooling rate which directly proportional to both the phase change rate and drift velocity. In order to understand this behavior, MAC values are plotted as a function of drift velocity in Fig. 7.

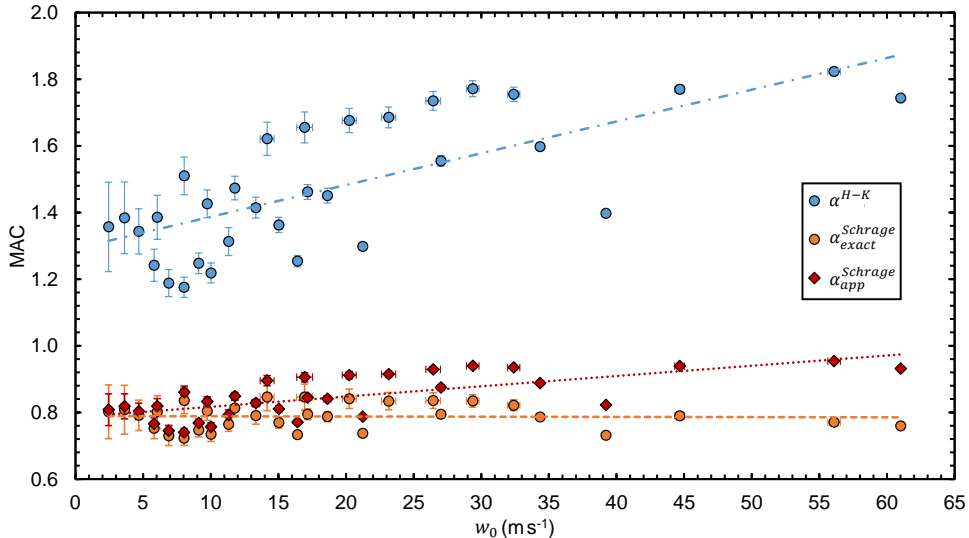


FIG. 7. Mass accommodation coefficients as a function of drift velocity during both near-equilibrium and non-equilibrium simulations. Dash, dot, and dash-dot lines are the linear fits to the data of MACs calculated based on exact Schrage relation, approximate Schrage relation and H-K equation, respectively.

Linear fits to the scattered data reveal that MAC values calculated from H-K equation and approximate Schrage relation increase with increasing drift velocity of the gas phase, whilst exact Schrage relation yields MAC values which do not exhibit considerable variation. Therefore, exact Schrage relation is able to adjust itself during a strong phase change process *via* the drift velocity correction factor utilized in the relation.

Tsurata *et al.* [11, 24] proposed a general expression for the condensation coefficient based on transition state theory. Comparison of MAC values of the current study with the ones obtained from the expression of Tsurata *et al.* is reported as the functions of both reduced temperature,  $T/T_c$ , and translational length ratio,  $(\rho^V/rho_i^L)^{1/3}$ , in Fig. 8. Mass accommodation coefficients calculated from exact Schrage relation is closest to the theoretical prediction. Coefficients calculated based on approximate Schrage relation is similar or slightly higher than the ones based on exact Schrage relation and they are not shown in Fig. 8 for brevity. Coefficients calculated based on H-K equation, on the other hand, almost double the predictions of transition state theory.

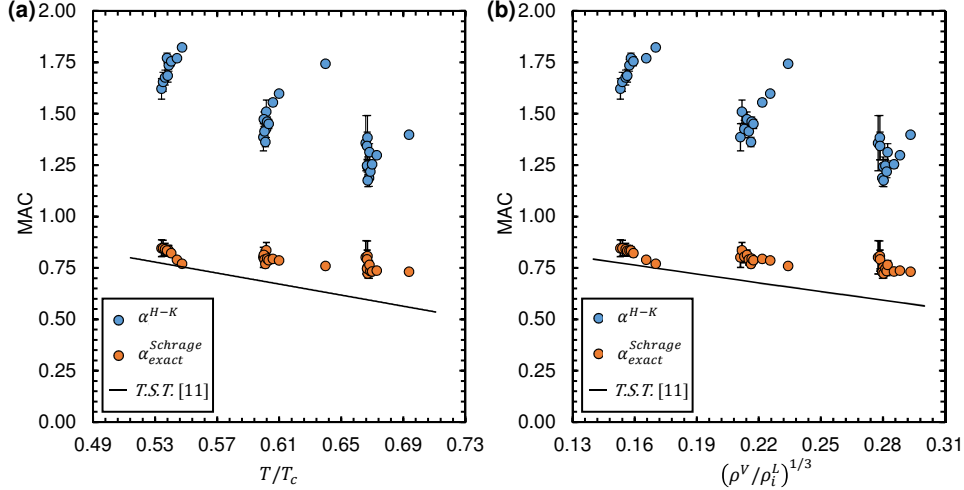


FIG. 8. Mass accommodation coefficients as the functions of (a) reduced temperature, and (b) translational length ratio. Solid lines show the predictions of transition state theory (T.S.T.). Critical temperature ( $T_c$ ) of argon is 150.86 K.

#### D. Effect of temperature rise near the interface

Possibility of an inverted temperature gradient during phase change first suggested in the theoretical study of Pao [76] in 1971. Fang and Ward [77] were first to report experimental evidence of a temperature discontinuity at an evaporating interface. Ward and Stanga [78] later reported the gas temperature rise near a condensing interface (i.e.  $T^V > T_i^V$ ). Subsequent MD studies [24, 79] were also able to demonstrate the inverted temperature profile between phase changing interfaces together with the warming of the gas phase near the condensing interface. During our simulations, temperature rise near the condensing interface together with the associated density drop [79] also exists as shown in Fig. 9. The temperature rise was attributed to the heat of evaporation in the study of Ytrehus [80]. The present study does not primarily aim to explain the underlying reason of the temperature rise. However, its effect on MAC values is of interest in this study.

Density and temperature of the gas phase utilized in Eqs. (12) and (13) are calculated by averaging the properties throughout bulk vapor phase. On the other hand, replacing  $T_V$  and  $\rho_V$  with  $T_i^V$  and  $\rho_i^V$  in Eqs. (12) and (13) can easily address the effect of temperature rise near the interface. However, temperature of the gas phase is inevitably subjected to fluctuations in the gas phase, which prevents us to determine an exact value at an exact position. Therefore, we averaged the data within enlarged bins (approximately equal to

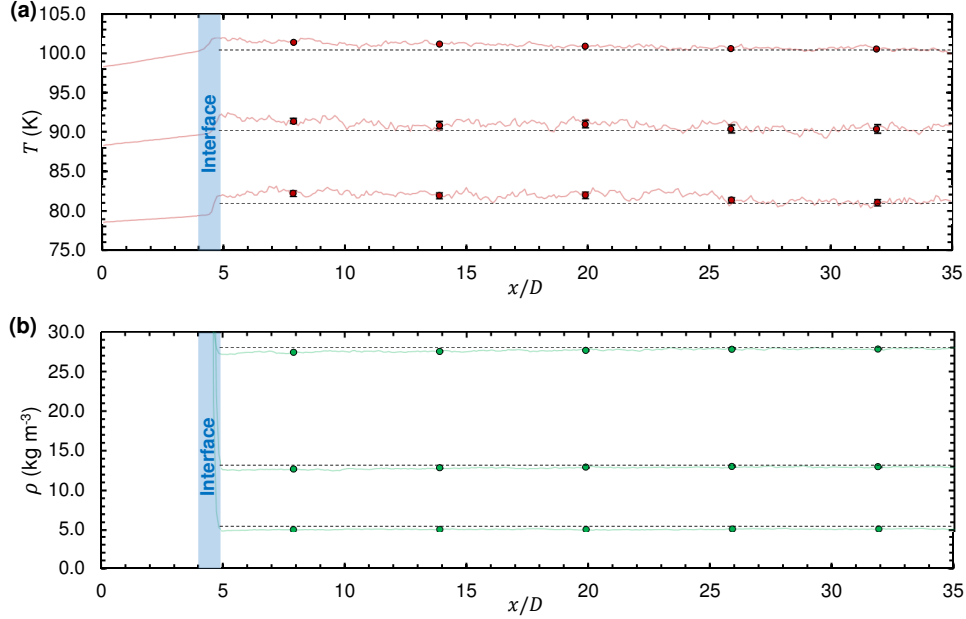


FIG. 9. Distributions of (a) temperature and (b) density of the gas phase near the interface. Semi-transparent solid lines show all the data. Circles show the data averaged within the intervals of 11.76 nm, which is nearly equal to the mean free path of an argon atom in gas phase around 90 K.

the mean free path of the gas) to eliminate the fluctuations as shown in Fig. 9. The data averaged in the nearest bin to the interface is used as the corresponding interfacial property ( $T_i^V$ ,  $\rho_i^V$ ). In other words, the interfacial properties were averaged values from within one mean free path in the vapor. Resultant MAC values together with the values calculated based on the bulk properties are shown in Fig. 10.

When the properties of gas near the interface are used instead of its bulk properties, MAC values have tendency to increase as shown in Fig. 10. The reason of this behavior is purely mathematical and can be understood when Eqs. (12) and (13) are examined. The temperature rise near the interface is offset by a reduction in density. Consequently, the values of MAC increase due to inverse proportionality with the terms in parenthesis. In an alternative point of view, since these terms actually represent the condensation rate of vapor ( $j^V$ ) as explained in Section I A, condensation probability is expected rise if the condensation rate ( $j^V$ ) increases with respect to the evaporation rate ( $j^L$ ).

The effect of utilizing near-interface properties of gas on the drift velocity dependence of MAC values is also investigated. Figure 11 shows the distribution of MAC values evaluated based on the properties of gas near the interface as a function of drift velocity. Similar

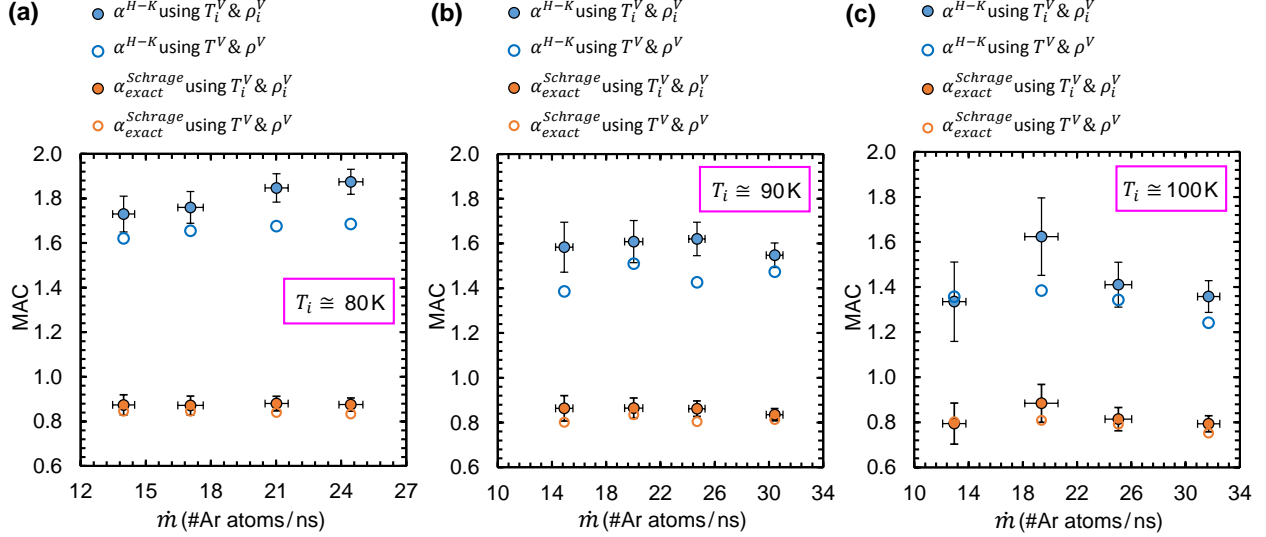


FIG. 10. Mass accommodation coefficients calculated based on the properties of gas within one mean free path distance from the interface. Coefficients are given as a function of condensation rate.

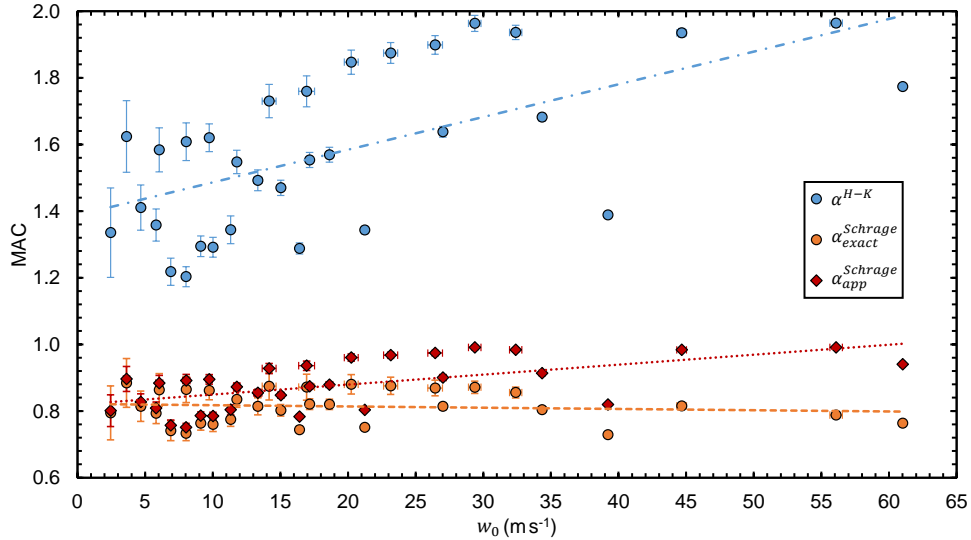


FIG. 11. Mass accommodation coefficients as a function of drift velocity during both near-equilibrium and non-equilibrium simulations, when the properties of gas near the interface are utilized. Dash, dot, and dash-dot lines are the linear fits to the data of MACs calculated based on exact Schrage relation, approximate Schrage relation and H-K equation, respectively.

to the trend of MAC values calculated on bulk gas properties (see Fig. 7), exact Schrage relation yields MAC values which do not exhibit considerable variation with increasing drift velocity. However, H-K equation and approximate Schrage relation still yield MAC values that increase with increasing drift velocity.

In this study, MAC was computed directly from the kinetic theory expressions. As the

name suggests, it is simply a coefficient that was originally introduced to make the equations match experimental data. In our case, we use the coefficient to match the equations with numerical simulation data. If there must exist an absolute need to define the coefficients, then care must be taken to set a standard definition that is both consistent with kinetic theory of phase change and is accompanied by a physical description of the location of  $S$  and  $S^*$  (see Fig. 2). We recommend the following definitions: the condensation coefficient ( $\alpha_c$ ) is the ratio of molecules that undergo condensation to the number of molecules that cross the hypothetical surface ( $S^*$ ) toward the bulk liquid. The evaporation coefficient ( $\alpha_e$ ) is the ratio of number of vapor molecules that originate from the bulk liquid to the number of vapor molecules that cross the hypothetical surface ( $S^*$ ) toward the bulk vapor. Where  $S$  is the intersection of the bulk liquid and the interfacial region and  $S^*$  is the intersection of the bulk vapor and the interfacial region (see Fig. 2).

#### IV. SUMMARY AND CONCLUSION

Kinetic theory of phase change is reviewed from a fundamental standpoint and corresponding assumptions built into the most commonly used expressions for liquid-vapor phase change, Hertz-Knudsen (H-K) and Schrage relations, are discussed. Additional attention is provided to the departure from equilibrium, which alters the macroscopic vapor (drift) velocity and the corresponding kinetic theory relationships. The much disputed and controversial evaporation and condensation coefficients, commonly assumed equal and termed the mass accommodation coefficient (MAC) are discussed and inconsistencies in prior definitions are highlighted.

Using a steady state, non-equilibrium molecular dynamics (NEMD) simulation of a phase change driven nanopump originally developed by Akkus and Beskok [61], we investigated the condensation process at a flat liquid vapor interface. Instead of setting a definition for MAC *a priori*, the value is calculated directly from the kinetic theory relationships. The simulation data is used to calculate an explicit value of MAC from three different kinetic theory expressions: H-K equation ( $\alpha^{H-K}$ ), approximate Schrage equation ( $\alpha_{app}^{Schrage}$ ) and the exact Schrage equation ( $\alpha_{exact}^{Schrage}$ ). Simulations were conducted for a range of heating/cooling rates from 0.2 - 4.0 nW at temperatures with the system saturated at 80K, 90K, and 100K. The results are summarized below:

1.  $\alpha^{H-K}$  is generally above unity for all cases tested. Values greater than unity violate conservation laws with respect to most common physical definitions outside the kinetic theory framework.
2. MAC values from the Schrage expressions ( $\alpha_{app}^{Schrage}$  and  $\alpha_{app}^{Schrage}$ ) are between 0.8 and 0.9. The difference between  $\alpha_{app}^{Schrage}$  and the  $\alpha_{exact}^{Schrage}$  expressions collapses as the saturation temperature is increased from 80K to 100K.
3. MAC values from all expressions ( $\alpha^{H-K}$ ,  $\alpha_{app}^{Schrage}$  and  $\alpha_{exact}^{Schrage}$ ) decrease with saturation pressure but the temperature dependency of  $\alpha^{H-K}$  is nearly 6 times greater than the Schrage expressions.
4. As the heating/cooling rate is increased, the phase change rate and correspondingly, the drift velocity increases. There is no noticeable change in the  $\alpha_{exact}^{Schrage}$ . However,  $\alpha_{app}^{Schrage}$  deviates from  $\alpha_{exact}^{Schrage}$  as the drift velocity is increased.  $\alpha^{H-K}$  also increases with drift velocity but at a much greater rate.
5. When bulk parameters in the vapor are used instead of interfacial properties, the change in MAC is found to be small but noticeable.

It is certainly possible to use either the H-K equation or the Schrage equation to predict phase change but care must be taken to ensure that the right corresponding value of MAC be used. MAC values computed with one kinetic theory model cannot be used interchangeably with another. We urge that in the future when MAC values are discussed, the researcher also details the corresponding kinetic theory model along with the simplifications or explicitly state the physical definition used to characterize the coefficient without the aid of kinetic theory. If the latter method is used, it is important to note that the MAC values are then limited to just that particular definition and cannot be interchangeably used with MAC values from alternative definitions.

$\alpha^{H-K}$  is sensitive to the departure from equilibrium (variations in phase change rate and/or drift velocity) and additional correction factors must be employed. Further,  $\alpha^{H-K}$  may be  $> 1$  and violate conservation laws when analyzed using a physical definition outside the kinetic theory framework. For these reasons, we recommend that the exact Schrage model be used whenever possible since departure from equilibrium (drift velocity) is inher-

ently accounted for.  $\alpha_{exact}^{Schrage}$  is unlikely to be  $> 1$  and thereby unlikely to violate conservation laws when definitions outside the kinetic theory framework are used.

## REFERENCES

---

- [1] S. Chapman, T. G. Cowling, and D. Burnett, *The mathematical theory of non-uniform gases: an account of the kinetic theory of viscosity, thermal conduction and diffusion in gases* (Cambridge University Press, 1990).
- [2] V. P. Carey, *Liquid vapor phase change phenomena: an introduction to the thermophysics of vaporization and condensation processes in heat transfer equipment* (CRC Press, 2018).
- [3] A. P. Kryukov and V. Y. Levashov, “About evaporation–condensation coefficients on the vapor–liquid interface of high thermal conductivity matters,” *Int. J. Heat Mass Tran.* **54**, 3042–3048 (2011).
- [4] R. Marek and J. Straub, “Analysis of the evaporation coefficient and the condensation coefficient of water,” *Int. J. Heat Mass Tran.* **44**, 39–53 (2001).
- [5] A. H. Persad and C. A. Ward, “Expressions for the evaporation and condensation coefficients in the hertz-knudsen relation,” *Chem. Rev.* **116**, 7727–7767 (2016).
- [6] H. Hertz, “Ueber die verdunstung der flüssigkeiten, insbesondere des quecksilbers, im luftleeren raume,” *Ann. Phys.* **253**, 177–193 (1882).
- [7] R. W. Schrage, *A theoretical study of interphase mass transfer*, Ph.D. thesis, Columbia University Press (1953).
- [8] G. Standart and Z. Cihla, “Interphase transport processes. i. schrage’s theories,” *Collect. Czech Chem. C* **23**, 1608–1618 (1958).
- [9] K. Yasuoka and M. Matsumoto, “Evaporation and condensation at a liquid surface. i. argon,” *J. Chem. Phys.* **101**, 7904–7911 (1994).
- [10] M. Matsumoto and K. Yasuoka, “Evaporation and condensation at a liquid surface. ii. methanol,” *J. Chem. Phys.* **101**, 7912–7917 (1994).
- [11] G. Nagayama and T. Tsuruta, “A general expression for the condensation coefficient based on the transition state theory and molecular dynamics simulation,” *J. Chem. Phys.* **118**,

- 1392–1399 (2003).
- [12] R. Meland, A. Frezzotti, T. Ytrehus, and B. Hafskjold, “Nonequilibrium molecular-dynamics simulation of net evaporation and net condensation, and evaluation of the gas-kinetic boundary condition at the interphase,” *Phys. Fluids* **16**, 223–243 (2004).
- [13] K. Gu, C. B. Watkins, and J. Koplik, “Molecular dynamics simulation of the equilibrium liquid–vapor interphase with solidification,” *Fluid Phase Equilibr.* **297**, 77–89 (2010).
- [14] S. H. Algie, “Kinetic theories of evaporation,” *J. Chem. Phys.* **69**, 538–543 (1978).
- [15] I. W. Eames, N. J. Marr, and H. Sabir, “The evaporation coefficient of water: a review,” *Int. J. Heat Mass Tran.* **40**, 2963–2973 (1997).
- [16] M. Knudsen, “Maximum rate of vaporization of mercury,” *Ann. Phys.* **47**, 697–705 (1915).
- [17] T. K. Xia and U. Landman, “Molecular evaporation and condensation of liquid n-alkane films,” *J Chem. Phys.* **101**, 2498–2507 (1994).
- [18] M. Matsumoto, “Molecular dynamics of fluid phase change,” *Fluid Phase Equilibria* **144**, 307–314 (1998).
- [19] S. I. Anisimov, D. O. Dunikov, V. V. Zhakhovskii, and S. P. Malysenko, “Properties of a liquid–gas interface at high-rate evaporation,” *J. Chem. Phys.* **110**, 8722–8729 (1999).
- [20] R. Hołyst, M. Litniewski, and D. Jakubczyk, “A molecular dynamics test of the hertz–knudsen equation for evaporating liquids,” *Soft Matter* **11**, 7201–7206 (2015).
- [21] J. Barrett and C. Clement, “Kinetic evaporation and condensation rates and their coefficients,” *J. Colloid Interf. Sci.* **150**, 352–364 (1992).
- [22] P. Davidovits, D. R. Worsnop, J. T. Jayne, C. E. Kolb, P. Winkler, A. Vrtala, P. E. Wagner, Kulmala. M., K. E. J. Lehtinen, T. Vesala, and M. Mozurkewich, “Mass accommodation coefficient of water vapor on liquid water,” *Geophys. Res. Lett.* **31** (2004).
- [23] A. Morita, M. Sugiyama, H. Kameda, S. Koda, and D. R. Hanson, “Mass accommodation coefficient of water: molecular dynamics simulation and revised analysis of droplet train/flow reactor experiment,” *J. Phys. Chem. B* **108**, 9111–9120 (2004).
- [24] T. Tsuruta and G. Nagayama, “A microscopic formulation of condensation coefficient and interface transport phenomena,” *Energy* **30**, 795–805 (2005).
- [25] P. M. Winkler, A. Vrtala, R. Rudolf, P. E. Wagner, I. Riipinen, T. Vesala, K. E. J. Lehtinen, Y. Viisanen, and M. Kulmala, “Condensation of water vapor: Experimental determination of mass and thermal accommodation coefficients,” *J. Geophys. Res.-Atmos.* **111** (2006).

- [26] J. Voigtländer, F. Stratmann, D. Niedermeier, H. Wex, and A. Kiselev, “Mass accommodation coefficient of water: a combined computational fluid dynamics and experimental data analysis,” *J. Geophys. Res.* **112**, D20208 (2007).
- [27] S. Cheng, Lechman J. B., S. J. Plimpton, and G. S. Grest, “Evaporation of lennard-jones fluids,” *J. Chem. Phys.* **134**, 224704 (2011).
- [28] K. Yasuoka, M. Matsumoto, and Y. Kataoka, “Dynamics near a liquid surface: mechanisms of evaporation and condensation,” *J. Mol. Liq.* **65-66**, 329–332 (1995).
- [29] T. Tsuruta, H. Tanaka, and T. Masuoka, “Condensation/evaporation coefficient and velocity distributions at liquid–vapor interface,” *Int. J. Heat Mass Tran.* **42**, 4107–4116 (1999).
- [30] A. Røsjorde, S. Kjelstrup, D. Bedeaux, and B. Hafskjold, “Nonequilibrium molecular dynamics simulations of steady-state heat and mass transport in condensation. ii. transfer coefficients,” *J. Colloid Interf. Sci.* **240**, 355–364 (2001).
- [31] T. Tsuruta and G. Nagayama, “Molecular dynamics studies on the condensation coefficient of water,” *J. Phys. Chem. B* **108**, 1736–1743 (2004).
- [32] Z. Liang, T. Biben, and P. Keblinski, “Molecular simulation of steady-state evaporation and condensation: Validity of the schrage relationships,” *Int. J. Heat Mass Tran.* **114**, 105–114 (2017).
- [33] D. Fuster, G. Hauke, and C. Dopazo, “Influence of the accommodation coefficient on nonlinear bubble oscillations,” *J. Acoust. Soc. Am.* **128**, 5–10 (2010).
- [34] P. C. Wayner, Y. K. Kao, and L. V. LaCroix, “The interline heat-transfer coefficient of an evaporating wetting film,” *Int. J. Heat Mass Tran.* **19**, 487–492 (1976).
- [35] Michael Mozurkewich, “Aerosol growth and the condensation coefficient for water: A review,” *Aerosol Sci. Tech.* **5**, 223–236 (1986).
- [36] GT Barnes, “The effects of monolayers on the evaporation of liquids,” *Adv. Colloid Interfac.* **25**, 89–200 (1986).
- [37] P. C. Wayner, “The effect of interfacial mass transport on flow in thin liquid films,” *Colloid. Surface.* **52**, 71–84 (1991).
- [38] S. DasGupta, I. Y. Kim, and P. C. Wayner, “Use of the kelvin-clapeyron equation to model an evaporating curved microfilm,” *J. Heat Transf.* **116**, 1007–1015 (1994).
- [39] P. C. Wayner, “Intermolecular forces in phase-change heat transfer: 1998 kern award review,” *AIChE J.* **45**, 2055–2068 (1999).

- [40] J. L. Plawsky, M. Ojha, A. Chatterjee, and P. C. Wayner, “Review of the effects of surface topography, surface chemistry, and fluid physics on evaporation at the contact line,” *Chem. Eng. Commun.* **196**, 658–696 (2008).
- [41] R. Holyst, M. Litniewski, D. Jakubczyk, M. Zientara, and M. Woźniak, “Nanoscale transport of energy and mass flux during evaporation of liquid droplets into inert gas: computer simulations and experiments,” *Soft Matter* **9**, 7766–7774 (2013).
- [42] C. S. Wang, J. S. Chen, J. Shiomi, and S. Maruyama, “A study on the thermal resistance over solid–liquid–vapor interfaces in a finite-space by a molecular dynamics method,” *Int. J. Therm. Sci.* **46**, 1203–1210 (2007).
- [43] K. H. Do, S. J. Kim, and S. V. Garimella, “A mathematical model for analyzing the thermal characteristics of a flat micro heat pipe with a grooved wick,” *Int. J. Heat Mass Tran.* **51**, 4637–4650 (2008).
- [44] S. Du and Y. H. Zhao, “New boundary conditions for the evaporating thin-film model in a rectangular micro channel,” *Int. J. Heat Mass Tran.* **54**, 3694–3701 (2011).
- [45] L. Bai, G. Lin, and G. B. Peterson, “Evaporative heat transfer analysis of a heat pipe with hybrid axial groove,” *J. Heat Transf.* **135**, 031503 (2013).
- [46] Y. Akkuş and Z. Dursunkaya, “A new approach to thin film evaporation modeling,” *Int. J. Heat Mass Tran.* **101**, 742–748 (2016).
- [47] Y. Akkuş, H. I. Tarman, B. Çetin, and Z. Dursunkaya, “Two-dimensional computational modeling of thin film evaporation,” *Int. J. Therm. Sci.* **121**, 237–248 (2017).
- [48] O. Akdag, Y. Akkus, and Z. Dursunkaya, “The effect of disjoining pressure on the shape of condensing films in a fin-groove corner,” *Int. J. Therm. Sci.* **142**, 357–365 (2019).
- [49] M. Alipour and Z. Dursunkaya, “Limitations of matching condensing film profile on a micro fin with the groove: critical effect of disjoining pressure,” *Nanosc. Microsc. Therm.* **23**, 289–303 (2019).
- [50] E.J. Davis, “A history and state-of-the-art of accommodation coefficients,” *Atmos. Res.* **82**, 561–578 (2006).
- [51] K. Bellur, E. F. Médiçi, C. K. Choi, J. C. Hermanson, and J. S. Allen, “Multiscale approach to model steady meniscus evaporation in a wetting fluid,” *Phys. Rev. Fluids* **5**, 024001 (2020).
- [52] T. Ishiyama, T. Yano, and S. Fujikawa, “Molecular dynamics study of kinetic boundary condition at an interface between argon vapor and its condensed phase,” *Phys. Fluids* **16**,

- 2899–2906 (2004).
- [53] R. Hołyst and M. Litniewski, “Evaporation into vacuum: Mass flux from momentum flux and the hertz–knudsen relation revisited,” *J. Chem. Phys.* **130**, 074707 (2009).
- [54] A. Lotfi, J. Vrabec, and J. Fischer, “Evaporation from a free liquid surface,” *Int. J. Heat Mass Tran.* **73**, 303–317 (2014).
- [55] G. Nagayama, M. Takematsu, H. Mizuguchi, and T. Tsuruta, “Molecular dynamics study on condensation/evaporation coefficients of chain molecules at liquidvapor interface,” *J. Chem. Phys.* **143**, 014706 (2015).
- [56] T. Tsuruta, N. Sakamoto, and T. Masuoka, “Condensation process at liquid-vapor interface and condensation coefficient,” *Therm. Sci. Eng.* **3**, 85–90 (1995).
- [57] M. Matsumoto and Y. Kataoka, “Dynamic processes at a liquid surface of methanol,” *Phys. Rev. Lett.* **69**, 3782 (1992).
- [58] J. Yu and H. Wang, “A molecular dynamics investigation on evaporation of thin liquid films,” *Int. J. Heat Mass Tran.* **55**, 1218–1225 (2012).
- [59] Z. Liang and P. Koblinski, “Molecular simulation of steady-state evaporation and condensation in the presence of a non-condensable gas,” *J. Chem. Phys.* **148**, 064708 (2018).
- [60] B. Hafskjold and S. K. Ratkje, “Criteria for local equilibrium in a system with transport of heat and mass,” *J. Stat. Phys.* **78**, 463–494 (1995).
- [61] Y. Akkus and A. Beskok, “Molecular diffusion replaces capillary pumping in phase-change-driven nanopumps,” *Microfluid. Nanofluid.* **23**, 14 (2019).
- [62] Y. Akkus, A. Koklu, and A. Beskok, “Atomic scale interfacial transport at an extended evaporating meniscus,” *Langmuir* **35**, 4491–4497 (2019).
- [63] Y. Akkus, C. T. Nguyen, A. T. Celebi, and A. Beskok, “A first look at the performance of nano-grooved heat pipes,” *Int. J. Heat Mass Tran.* **132**, 280–287 (2019).
- [64] Y. Akkuş, “Modeling of evaporation from nanoporous membranes using molecular dynamics simulation,” *Isi Bilim Tek. Derg.* **39**, 91–99 (2019).
- [65] F. Heslot, N. Fraysse, and A. M. Cazabat, “Molecular layering in the spreading of wetting liquid drops,” *Nature* **338**, 640 (1989).
- [66] L. Cheng, P. Fenter, K. L. Nagy, M. L. Schlegel, and N. C. Sturchio, “Molecular-scale density oscillations in water adjacent to a mica surface,” *Phys. Rev. Lett.* **87**, 156103 (2001).
- [67] S. Yesudasan and S.C. Maroo, “Origin of surface-driven passive liquid flows,” *Langmuir* **32**,

- 8593–8597 (2016).
- [68] S. Maruyama and T. Kimura, “A study on thermal resistance over a solid-liquid interface by the molecular dynamics method,” *Therm. Sci. Eng.* **7**, 63–68 (1999).
- [69] S. M. Foiles, M. I. Baskes, and M. S. Daw, “Embedded-atom-method functions for the fcc metals Cu, Ag, Au, Ni, Pd, Pt, and their alloys,” *Phys. Rev. B* **33**, 7983 (1986).
- [70] M. Barisik and A. Beskok, “Boundary treatment effects on molecular dynamics simulations of interface thermal resistance,” *J. Comput. Phys.* **231**, 7881–7892 (2012).
- [71] S. Plimpton, “Fast parallel algorithms for short-range molecular dynamics,” *J. Comput. Phys.* **117**, 1–19 (1995).
- [72] J. R. D. Copley and S. W. Lovesey, “The dynamic properties of monatomic liquids,” *Rep. Prog. Phys.* **38**, 461 (1975).
- [73] A. Røsørde, D. W. Fossmo, D. Bedeaux, S. Kjelstrup, and B. Hafskjold, “Nonequilibrium molecular dynamics simulations of steady-state heat and mass transport in condensation: I. local equilibrium,” *J. Colloid Interf. Sci.* **232**, 178–185 (2000).
- [74] T.Q. Vo, M. Barisik, and B.H. Kim, “Near-surface viscosity effects on capillary rise of water in nanotubes,” *Phys. Rev. E* **92**, 053009 (2015).
- [75] J. Ghorbanian, A. T. Celebi, and A. Beskok, “A phenomenological continuum model for force-driven nano-channel liquid flows,” *J. Chem. Phys.* **145**, 184109 (2016).
- [76] Y. Pao, “Application of kinetic theory to the problem of evaporation and condensation,” *Phys. Fluids* **14**, 306–312 (1971).
- [77] G. Fang and C. A. Ward, “Temperature measured close to the interface of an evaporating liquid,” *Phys. Rev. E* **59**, 417 (1999).
- [78] C. A. Ward and D. Stanga, “Interfacial conditions during evaporation or condensation of water,” *Phys. Rev. E* **64**, 051509 (2001).
- [79] A. Frezzotti, P. Grosfils, and S. Toxvaerd, “Evidence of an inverted temperature gradient during evaporation/condensation of a lennard-jones fluid,” *Phys. Fluids* **15**, 2837–2842 (2003).
- [80] T. Yttrhus, “Molecular-flow effects in evaporation and condensation at interfaces,” *Multiphase Science and Technology* **9** (1997).